

# Experimental and Computational Investigation of Wake-Induced Vibration

J. F. Derakhshandeh, M. Arjomandi, B. Cazzolato and B. Dally

School of Mechanical Engineering  
University of Adelaide, Adelaide, South Australia 5005, Australia

## Abstract

The use of non-turbine systems to generate hydropower energy has drawn the attention of researchers. In the current paper, Wake Induced Vibration (WIV) is experimentally and numerically studied. For this purpose, two circular cylinders were arranged in a tandem in a water channel; the upstream cylinder was fixed and the downstream one was supported by a virtual elastic base. Force and displacement measurements were conducted on the downstream cylinder in a transitional flow regime,  $Re = 2,000-15,000$ . The effects of the longitudinal and lateral distances between the cylinders on the dynamic response of the WIV were investigated. It is shown that WIV can occur outside the frequency of the Vortex Induced Vibration (VIV), resulting in a higher potential of energy harnessing. The results reveal that the efficiency of power generation from WIV depends on the position of the downstream cylinder, and it is a function of the Reynolds number. In addition, Computational Fluid Dynamic (CFD) studies were performed using a Scale Adaptive Simulation (SAS) model to analyse the flow characteristics around the cylinders. The lift, displacement amplitude and frequency of oscillation calculated by the numerical modelling are in a reasonable agreement with the experimental data.

## Introduction

Increases in energy demand and global warming have motivated scholars to investigate new renewable and environmentally friendly energy generation technologies. Vortex Induced Vibrations (VIVs) is one such technology (Bernitsas and Raghavan 2004). The term of VIVs denotes to those phenomenon associated with the reaction of structures in a cross flow. There are numerous studies in the literature with a focus on the VIV phenomenon of a circular cylinder. Bernitsas *et al.* (2008) developed a converter to capture VIV energy generated from ocean currents. In their studies, the experimental and theoretical VIV efficiencies were estimated to be 22% and 37%, respectively. The response of a cylinder to VIV was modelled using a Mass-Spring-Damper (MSD) by Bearman (1984) and following his proposed model, Hover *et al.* (1997) offered the first computer model of Virtual Mass-Spring-Damper (VMSD). The VMSD system allows the operator to electronically set the desired impedance of the MSD. This facilitates the rapid examination of a wide range of experimental test cases rapidly compared to the physical MSD, which requires replacing the parts of the system to change the impedance.

Using the VMSD models opened the way for optimisation and further investigation of energy utilization. In spite of the extensive studies on VIV of a cylinder, Wake Induced Vibration (WIV) has not received similar attention, particularly to harness kinetic energy of free streams in shallow rivers or oceanic currents. In the WIV mechanism, when the downstream cylinder is displaced sideways, a lift force would act to move the cylinder towards the centreline (Zdravkovich 1977). The most comprehensive study on this field was conducted by Assi (2009), who studied the WIV mechanism of two similar cylinders and reported the dynamic response of the downstream one at a range of Reynolds number between 1,000 and 30,000. It was observed that the WIV response of the cylinder is a function of

longitudinal distance between the cylinders. In the current paper, a new design for a VMSD mechanism is presented. For this purpose, a vertically mounted cylinder in a cross-flow was utilized, as opposed to previous work, which employed a horizontally positioned cylinder. This approach eliminates the effect of weight and buoyancy forces on the drive mechanism, and consequently improves the accuracy of the data. In addition, besides the VIV effect, the WIV response of an elastic cylinder is considered for harnessing the hydrokinetic energy of the wake. In the WIV, the maximum amplitude of oscillation is not limited to the resonance frequency of the structure, which facilitates the capture of energy from the vortices outside the natural frequency of the structure.

## Experimental details

To investigate the effect of the arrangement of two circular cylinders on the efficiency of the WIV power, a series of tests were conducted in a closed-loop water channel with a test section of 2,000 mm length, 500 mm wide, and 600 mm depth at the University of Adelaide. Two cylinders with different diameters were employed. The upstream cylinder had a diameter of  $D_1 = 40$  mm and length of 600 mm and was stationary at a fixed position during the experiment. The downstream cylinder had a smaller diameter of  $D_2 = 30$  mm and length of 400 mm. This cylinder was mounted on the elastic base of the VMSD system. The longitudinal ( $x_0$ ) and lateral ( $y_0$ ) distances between the cylinders were varied as shown in figure 1. A total of sixteen arrangements of the cylinder were tested. The flow velocity was varied between 0.05 m/s and 0.37 m/s and consequently the maximum Reynolds number achieved, based on the density of water and the diameter of the upstream cylinder, was  $Re=15,000$ .

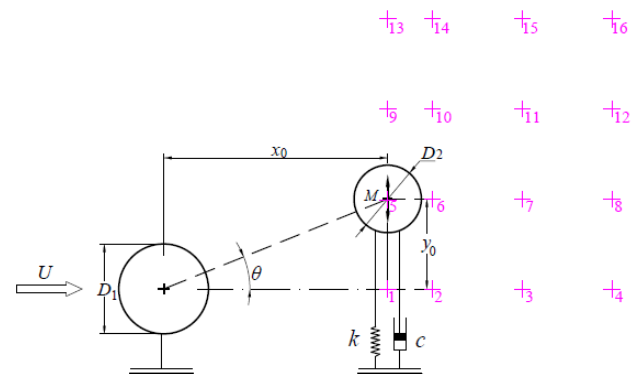


Figure 1. Schematic of the arrangements of the elastically mounted cylinder relative to the stationary upstream cylinder. Sixteen test cases are considered. (+) symbols denote the position of the centre of the downstream cylinder.

## Virtual Mass Spring damper (VMSD) and Proportional Integral Derivative (PID) control system

The VMSD used in the experiments consisted of a Maxon brushless EC-Max 30 (with 2,000 quad-count encoder) servo-motor, a gearbox of 51:1 ratio, two toothed pulleys and toothed belt which were attached to a carriage running on four linear bearings. In order to control the servo-motor a Maxon ESCON

50/5 servo controller was used. The fluidic force in normal direction to the mean flow, exerted on the downstream cylinder, was measured using two strain gauges in a half-bridge arrangement. The bridge directly measured the moment at the root of the cantilevered column, and by assuming 2D flow conditions; the lateral force was estimated. The corresponding equipment and the water channel test section are shown in figure 2. The instantaneous displacement of the downstream cylinder was measured and controlled using a Proportional-Integral-Derivative (PID) controller. The pulses generated by the embedded encoder in the Maxon motor were used for measuring the angular position of the motor shaft as well as speed (angular velocity). The position signal of the motor was used for feedback control. The angle of rotation of the shaft was converted to the real linear displacement of the carriage to which the cylinder was attached. As a result, the difference between measured oscillation of the downstream cylinder and equivalent linear displacement of the shaft was calculated as an error value. This value was defined as an input signal of the PID controller. The PID controller is tuned using Ziegler Nichols method (Astrom and Hagglund 2006).

The proportional, integral and derivative gains of PID controller set to minimize the output error of displacement to less than 1 mm. Compared with amplitude of oscillation of the cylinder, this small discrepancy was negligible.

The dSPACE software was used for the real time communication with the nonlinear PID controller and data acquisition. Despite the high flexibility of the VMSD system, by setting various mass and damping ratios using the Simulink software, in the current study, the mass and damping ratios were kept constant in order to study the influence of the geometry and Reynolds number on the efficiency of the WIV power. In addition, to facilitate the comparison of the results with the previously published data (Assi 2009), the mass and damping ratios were kept constant at 2.4 and 0.01, respectively, and the Reynolds number was changed from 2,000 to 15,000 by adjusting the free stream velocity of the water channel.

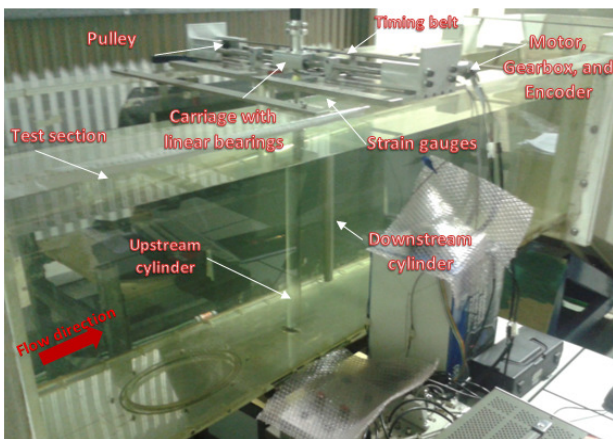


Figure 2. Experimental setup showing the water channel, the cylinders and the VMSD model for force and displacement measurements.

## Results and discussion

A series of force and displacement measurements were conducted in order to analyse the dynamic response of the downstream cylinder as a function of the cylinders' arrangement and the Reynolds number. In order to assess the accuracy of the VMSD system, a similar arrangement to the previously published work of Assi (2009) was chosen and the dimensionless amplitude

of oscillation of the downstream cylinder was compared (see figure 1, Test case 3). Herein, the amplitude of oscillation is normalized by the diameter of the downstream cylinder ( $Y^*$ ). As shown in figure 3, the displacement of the cylinder is in a good agreement with the published data by Assi (2009) for  $Re < 13,000$ . The small discrepancy between the data can be due to different experimental methods, and is within acceptable bounds for experimental reproducibility

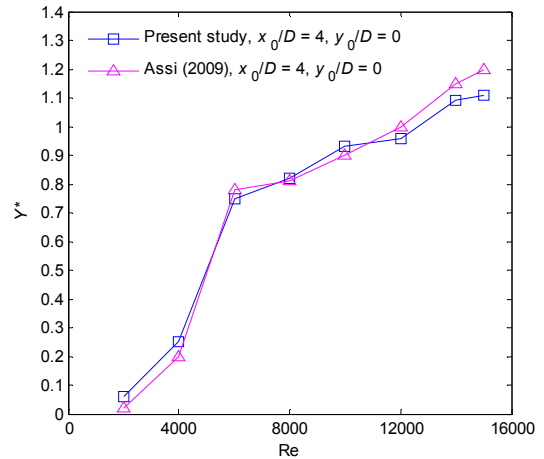


Figure 3. Comparison of the dimensionless amplitude displacement as a function of the Reynolds number with the published data by Assi (2009).

Figure 4 shows the effect of both longitudinal and lateral distances between the cylinders on the amplitude of oscillation of the downstream cylinder. As shown in the figure, the minimum and maximum displacement amplitude occur at the conditions of Test cases 1 and 11, respectively. These two test cases are marked by the lower ( $\nabla$ -) and upper ( $\Delta$ -) bounds. The amplitude of oscillation of the other test cases was found to be within these two bounds. It is observed that for lower Reynolds numbers,  $Re \leq 6,000$ , the lateral distance between cylinders has a larger effect on the displacement amplitude of the downstream cylinder, which has been not reported previously. It is also observed that with an increase in longitudinal distance between cylinders from  $x_0/D_1 = 2.5$  to 4 (Test Case 1 and 11, respectively), the displacement amplitude increases, which is agreement with Assi's work (2009), who showed that among those test cases with  $4 \leq x_0/D_1 \leq 20$ , the maximum displacement amplitude of the cylinder is achievable for  $x_0/D_1 = 4$ . The maximum displacement of the downstream cylinder was compared with the VIV response of a single cylinder in order to highlight the response of the WIV mechanism in harnessing the hydrokinetic energy. Figure 5 presents the displacement amplitudes of the VIV of a single cylinder, which referred to the initial, upper and lower branches in the literature (Williamson and Roshko 1988). Here, these responses are categorised into three zones; known as Zone 1, Zone 2 and Zone 3. In Zone 1, the WIV amplitude achieved for the staggered arrangements is higher than that of the VIV amplitude of a single cylinder. However, in Zone 2 the maximum achievable amplitude of the WIV is lower than amplitude of the VIV. It is also observed that for the staggered arrangement of the cylinders, Zone 3 shows much higher displacement amplitude compared with the one of the VIV. It is also worth noting that in Zone 3 the maximum amplitude of displacement is higher than the upper branch of the VIV response of a single cylinder in Zone 2. Thus, in contrast to the VIV, it is shown that the maximum amplitude of oscillation in the WIV is not limited to the natural frequency of the cylinder, and by increasing the Reynolds number the amplitude of oscillation increases.

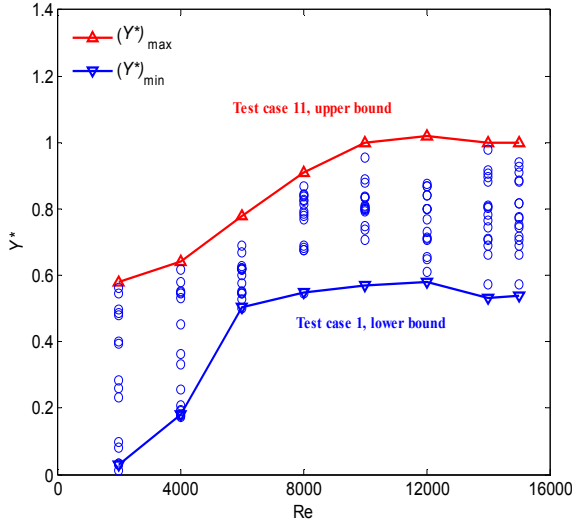


Figure 4. Scatter plot of all tests cases comprising the upper and lower bounds (Test case 11 and 1, respectively) as a function of the Reynolds number, and the lateral and the longitudinal distances between cylinders. Circles represent different arrangements.

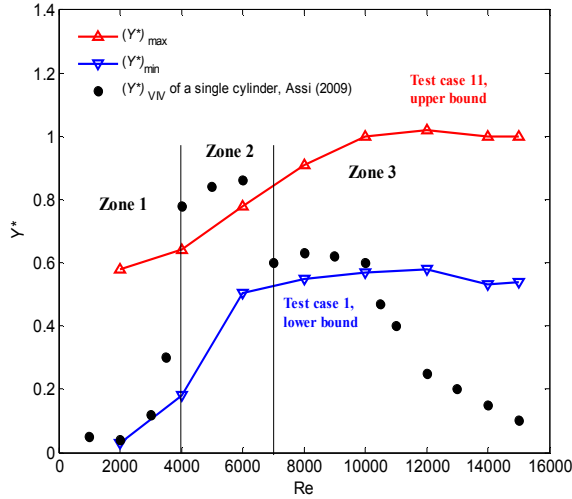


Figure 5. Comparison of the WIV response of the downstream cylinder and the VIV of a single cylinder as a function of the Reynolds number.

The fluid power was applied to compute the efficiency of the power and it can be formulated as  $P_{\text{fluid}} = FU = (\frac{1}{2})\rho U^3 D_2 L$ , therefore,

$$\eta_{\text{WIV}} = \frac{P_{\text{WIV}}}{P_{\text{fluid}}} \quad (1)$$

In above Equation  $P_{\text{WIV}}$  is the average power, which is given by

$$P_{\text{WIV}} = \frac{W_{\text{WIV}}}{T}, \quad (2)$$

where,  $W_{\text{WIV}}$  is integrating the inner product of the force and the instantaneous velocity, and can be calculated over a complete cycle of oscillation ( $T$ ) as follow

$$W_{\text{WIV}} = \int_0^T F_y \dot{y} dt. \quad (3)$$

In figure 6 the isolines contours of the WIV efficiency are plotted as a function of longitudinal ( $x_0/D_1$ ) and lateral ( $y_0/D_1$ ) distances between cylinders at Reynolds number 6,000. It is observed that the highest WIV efficiency of 28% is obtained for the cases in which the downstream cylinder is positioned at  $3.5 \leq x_0/D_1 \leq 4.5$  and  $1 \leq y_0/D_1 \leq 2$ .

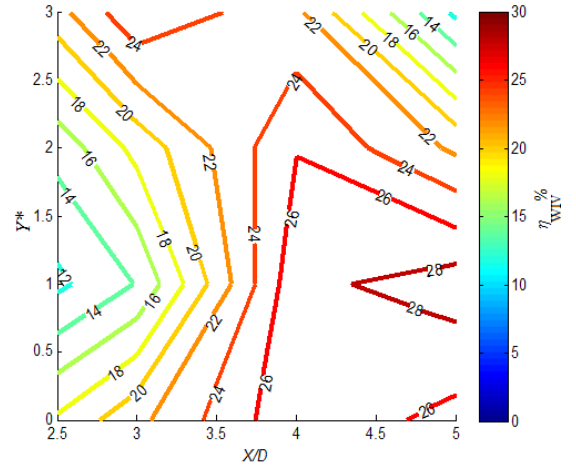


Figure 6. Effect of arrangement of the cylinders on the efficiency of WIV power ( $\eta_{\text{WIV}}\%$ ). Isolines contours of the WIV efficiency versus longitudinal and lateral position of the downstream cylinder at  $Re = 6000$ .

### Computational Fluid Dynamic Study

In order to investigate the flow pattern and study the characteristics of the flow, a Scale Adaptive Simulation (SAS) turbulence model was used to model a transitional flow regime over two circular cylinders. In comparison to the other turbulence models of Reynolds Average Navier Stokes (RANS) and Large Eddy Simulation (LES), the SAS model uses the von Karman length scale, which is defined as (Mentor and Egorov 2005)

$$L_{vk} = k_t \left| \frac{\partial U / \partial y}{\partial^2 U / \partial y^2} \right|. \quad (4)$$

Here,  $k_t$  is the turbulent kinetic energy. The von Karman length scale enables the model to adapt its behaviour to Scale Resolving Simulation (SRS) according to the stability parameters of the flow. This allows the model to provide a balance between the contributions of the simulated and resolved parts of the turbulence stresses. The SAS model was successfully examined in the previous works by the authors (Derakhshandeh *et al.* 2014-a, and 2014-b) and its reliability for this study was demonstrated. Figure 7 shows a 2D computational domain and the structured mesh elements in the computational domain and around the cylinders.

The vortex pattern in the wake of the cylinders is shown in figure 8. It can be seen that the vortex pattern of the upstream and downstream cylinders are “2S” and “2P”, respectively. The term 2S means that in each half-cycle a vortex is shed, similar to the natural Karman vortex shedding, while the term 2P highlights the formation of vortex pairs, which transfer with the flow at an angle outwards from the wake centreline. These two types of vortex patterns are known as the major vortex patterns in which the resonance or lock-in occurs compared with P or S modes of vortex patterns (Williamson and Roshko, 1988). With the 2S and 2P vortex generation modes, a synchronisation of oncoming vortices (2S) occurs with the vortices of the downstream cylinder. As a result, stronger circulation is produced which is directly proportional to the lift force acting on the downstream cylinder and causes a higher displacement. Therefore, the generated vortex pattern can considerably affect the dynamic response of the downstream cylinder when the cylinder is located in a reasonable lateral distance of the upstream cylinder.

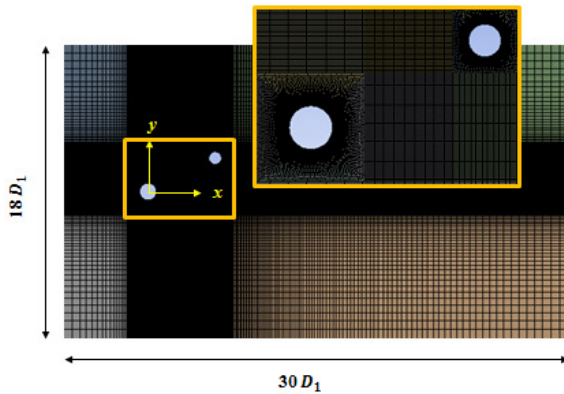


Figure 7. Quadrilateral mesh grid around two circular cylinders and the dimensions of computational domain.

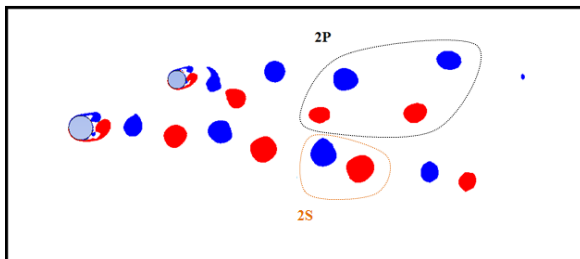


Figure 8. Contours of the vortex formation in the wake of the cylinders at  $Re = 6,000$  including vortex modes. The upstream cylinder is stationary and the downstream cylinder is elastically mounted.

## Conclusions

Experimental and numerical investigations were implemented to assess the WIV. For the experimental part, a Virtual Mass Spring Damper (VMSD) system was designed and employed. Force, displacement and frequency measurements were conducted in a closed-loop water channel using a Maxon motor and strain gauges all linked to a computer by a dSPACE control system. As the cylinders were installed vertically in the test section, the effect of gravity and buoyancy were considered negligible, hence the non-linearities observed on previous works were successfully removed. It was shown that in the VIV mechanism the upper branch of amplitude occurs at a limited range of frequencies (or reduced velocities) in which the shedding frequency is very close to the resonance frequency of the structure. However, for the staggered arrangement of the cylinders, the results show that WIV responses can occur at the frequencies outside the range in which VIV is observed. The staggered arrangement of the cylinders results in increased WIV efficiency (up to 28%) as compared to the aligned arrangement of the cylinders. The results of water channel tests also showed that of sixteen test cases the staggered arrangement with  $3.5 \leq x_0/D_1 \leq 4.5$  and  $1 \leq y_0/D_1 \leq 2$  showed the highest efficiency of the WIV power. The present experimental results showed that the Reynolds number plays an important role on the efficiency of the WIV energy. The alteration of the Reynolds number changes the upstream vortex shedding frequency which affects the phase difference of the lift and displacement of the downstream cylinder, subsequently impacting the WIV efficiency. Numerical analysis also demonstrates that for flow around two circular cylinders, when the downstream one is based on an elastic support, the mode of oncoming and downstream vortices are 2S and 2P, respectively. These modes are known as the major vortex pattern for a vibrated cylinder (Williamson and Roshko, 1988), in which the synchronisation occurs. Therefore, based on the arrangement of

the cylinders, the dynamic response of the downstream cylinder can be different.

## References

- [1] Assi, G., Mechanisms for flow-induced vibration of interfering bluff bodies. PhD thesis, Imperial College London, London, UK, 2009.
- [2] Astrom, K.J. and T. Hagglund, Advanced PID Control. ISA, 2006.
- [3] Bernitsas, M.M. & Raghavan, K., Converter of current/tide/wave energy. Provisional Patent Application. United States Patent and Trademark Office Serial, 2004, Serial No. 60/628,252.
- [4] Bernitsas, M.M., Raghavan, K., Ben-Simon, Y. & Garcia, E., VIVACE (Vortex Induced Vibration Aquatic Clean Energy): A new concept in generation of clean and renewable energy from fluid flow. Journal of Offshore Mechanics and Arctic Engineering, 2008, 130, 1-15.
- [5] Bearman, P.W., Vortex shedding from oscillating bluff bodies. Fluid Mechanics, 1984, 16, 195-222.
- [6] Blevins, R.D., Flow-induced vibration. Krieger publishing company, Malabar, Florida, USA, 1990.
- [7] Derakhshandeh, J.F., Arjomandi, M., Dally, B. & Cazzolato, B., Effect of a rigid wall on the vortex induced vibration of two staggered circular cylinders, Journal of Renewable and Sustainable Energy, 2014-a, 6, 033114.
- [8] Derakhshandeh, J.F., Arjomandi, M., Dally, B. & Cazzolato, B., The effect of arrangements of two circular cylinders on the maximum efficiency of Vortex-Induced Vibration power using a Scale Adaptive Simulation model, Journal of Fluids and Structures, 2014-b, 10.1016.
- [9] Hover, F., S. Miller, & M. Triantafyllou, Vortex-induced vibration of marine cables: Experiments using force feedback. Journal of Fluids and Structures, 1997, 11(3), p. 307-326.
- [10] Menter, F. & Egorov, Y., A scale-adaptive simulation model using two-equation models. 43rd AIAA Aerospace Sciences Meeting and Exhibit 1-13, 2005.
- [11] Williamson, C. & Roshko, A., Vortex formation in the wake of an oscillating cylinder. Journal of Fluids and Structures, 1988, 2 (4), 355-381.
- [12] Zdravkovich, M., 1st edition, Flow Around Circular Cylinders, vol. 1. Oxford University Press Inc., New York, 1997.